European Journal of Medicinal Chemistry 46 (2011) 3302–3308

Contents lists available at ScienceDirect

European Journal of Medicinal Chemistry

journal homepage: http://www.elsevier.com/locate/ejmech

Original article

Cytotoxic oxasqualenoids from the red alga *Laurencia viridis*

Francisco Cen-Pacheco [a], Janny A. Villa-Pulgarin [b,c], Faustino Mollinedo [b], Manuel Norte [a], Antonio H. Daranas [a,*], José J. Fernández [a,*]

[a] Instituto Universitario de Bio-Orgánica "Antonio González", Universidad de la Laguna, Astrofísico Francisco Sánchez 2, 38206 La Laguna, Tenerife, Spain
[b] Instituto de Biología Molecular y Celular del Cáncer, Centro de Investigación del Cáncer, CSIC-Universidad de Salamanca, Campus Miguel de Unamuno, E-37007 Salamanca, Spain
[c] APOINTECH, Centro Hispano-Luso de Investigaciones Agrarias (CIALE), Parque Científico de la Universidad de Salamanca, C/ Rio Duero 12, E-37185 Villamayor, Salamanca, Spain

ARTICLE INFO

Article history:
Received 3 March 2011
Received in revised form
18 April 2011
Accepted 19 April 2011
Available online 29 April 2011

Keywords:
Oxasqualenoids
Marine polyether
Laurencia
Integrin inhibitor

ABSTRACT

Three new polyether squalene derivatives 15-dehydroxythyrsenol A (**2**), prethyrsenol A (**3**) and 13-hydroxyprethyrsenol A (**4**) have been isolated from the red alga *Laurencia viridis*. Their structures were determined through the interpretation of NMR spectroscopic data and chemical correlations. In addition, four semi-synthetic compounds modulating the solubility of the lead compound dehydrothyrsiferol (**1**) were prepared without loss of activity. The cytotoxicity of the new compounds exhibited low μM activities. In order to explain their biological properties, docking simulations of the natural and synthetic compounds onto the αvβ3 integrin binding region were carried out.

1. Introduction

Natural products have played a fundamental role in biomedical research and drug development during the last decades, either directly as drugs or as lead structures that were further optimized by medicinal chemists. Within the wide range of natural sources marine organisms have become the most prolific producers of novel structures. In fact, many marine natural products have already undergone clinical trials as a result of their interesting pharmacological properties [1–4]. Within this chemical arsenal, molecules with exciting biological activities include polyether compounds, such as the squalene-derived metabolites isolated from the red alga *Laurencia*. In fact, a large number of triterpenic polyether compounds with significant structural and pharmacological diversity have been identified. Within this family, dehydrothyrsiferol (**1**), can be considered as a lead compound with moderate to potent cytotoxic activity, depending on the cellular lines used in the assay [5,6]. More interestingly, the identified molecular targets for dehydrothyrsiferol (**1**) and their congeners include the Ser-Thr Protein phosphatase type 2A (PP2A) [7], and some integrins [8]. Integrins are cell surface α-β-heterodimers, involved in cell–cell and cell–matrix interactions, with bidirectional signalling properties [2,7]. Several findings support participation of integrins in tumorigenesis and metastasis formation, suggesting that their regulation could be of real therapeutic potential in anticancer therapy.

Report herein is the isolation and structure elucidation, as well as the cytotoxic and PP2A inhibitory effects, of three new *Laurencia viridis* natural products and four semi-synthetic compounds derivated from **1**.

2. Chemistry

Fresh algal material (*L. viridis*) was extracted using $CHCl_3$:MeOH (1:1) at room temperature, and the resulting extract was successively subjected to sequential Sephadex LH-20, silica gel, Lichroprep and μ-Porasil column chromatographies to afford three new polyether compounds **2**–**4** (Fig. 1). Afterwards, their structures were established on the basis of their spectroscopical data.

The first isolated compound was closely related to the previously known thyrsenol A (**5**) [9] and it was identified as 15-dehydroxythyrsenol A (**2**), according to its molecular formula $C_{30}H_{51}O_7Br$ (HRESI-MS m/z 602.2810 and 604.9633) and NMR data (Table 1). Comparison of the ^1H and ^{13}C chemical shifts for both compounds pointed out the absence of the tertiary alcohol at C-15 in **5** (δ_C = 85.5), which was substituted by a methine (δ_H = 2.07; δ_C = 28.2) in **2**. The high chemical shifts coincidence in both compounds lead us to the conclusion that the configurations of all

* Corresponding authors. Tel.: +34922318586; fax: +34922318571.
E-mail addresses: adaranas@ull.es (A.H. Daranas), jjfercas@ull.es (J.J. Fernández).

0223-5234/$ – see front matter © 2011 Elsevier Masson SAS. All rights reserved.
doi:10.1016/j.ejmech.2011.04.051

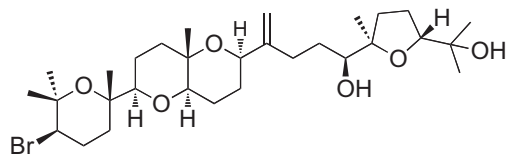

1 Dehydrothyrsiferol

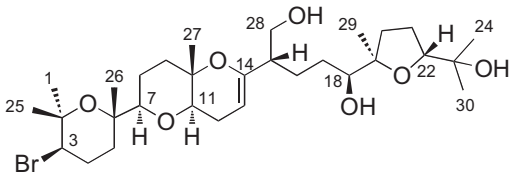

2 15-Dehydroxythyrsenol A

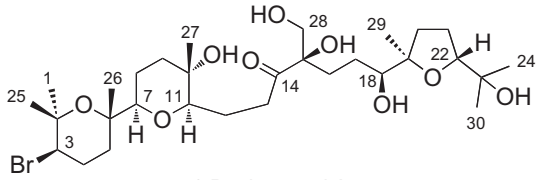

3 Prethyrsenol A

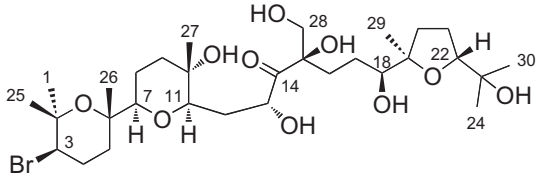

4 13-Hydroxyprethyrsenol A

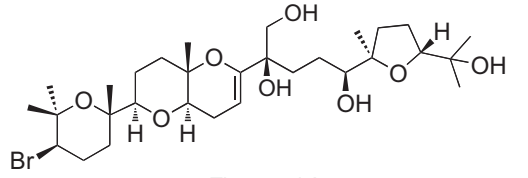

5 Thyrsenol A

Fig. 1. Chemical structures of the new metabolites isolated from *Laurencia viridis* (**2**–**4**) as well as of the lead compounds **1** and **5**.

quiral centres in **2** should be identical to those reported for **5**, with the exception of C-15 that should be now *S**, as a consequence of the change in substituent priority according to the Cahn-Ingold-Prelog rules. This was confirmed by a detailed analysis of the observed ROESY correlations, in particular those connecting H-3 (δ_H 3.89) with H_3-1 (δ_H 1.27), H-4α (δ_H 2.12) and H-5α (δ_H 1.52); H_3-25 (δ_H 1.40) with H-5β (δ_H 1.81) and H_3-26 (δ_H 1.21) as well as H-7 (δ_H 3.08) and H-11 (δ_H 3.31) with H_3-27 (δ_H 1.07) and H-8β (δ_H 1.50) together with the absence of correlation between H_3-29 (δ_H 1.29) with H-22 (δ_H 3.76). These data indicated that the relative configurations at the A, B, C and D rings are identical to those observed in tirsenol A (**5**). The *S** configuration at C-15 was proposed on the basis of ROE correlations between H-13 (δ_H 5.03) with H-16 (δ_H 1.81), H_3-27 (δ_H 1.07), H-28 (δ_H 3.63) and H_3-29 (δ_H 1.23), and H-16 (δ_H 1.81) with H_2-28 (δ_H 3.49 and 3.63). In addition, a Monte Carlo conformational search of **2** with the proposed relative configuration produced a conformer that matches the experimental data (see SI).

Table 1
NMR Chemical shifts for compounds **2**–**4** (in $CDCl_3$, 298 K).

	15-Dehydroxythyrsenol A (**2**)		Prethyrsenol A (**3**)		13-Hydroxyprethyrsenol (**5**)	
	δ ^{13}C	δ ^{1}H	δ ^{13}C	δ ^{1}H	δ ^{13}C	δ ^{1}H
1	31.0	1.27 (3H)	31.0	1.26 (3H)	31.0	1.27 (3H)
2	75.1		74.9		75.0	–
3	59.0	3.89	58.8	3.88	58.9	3.88
4	28.2	(α)2.12/2.24(β)	28.2	(α)2.07/2.25(β)	28.2	(α)2.10/2.24(β)
5	37.0	(α)1.52/1.81(β)	36.9	(α)1.54/1.78(β)	36.6	(α)1.63/1.76(β)
6	74.5		74.5		74.4	–
7	86.4	3.08	86.1	2.95	86.1	3.04
8	23.6	(β)1.50/1.82(α)	23.4	(β)1.37/1.74(α)	23.5	(β)1.39/1.75(α)
9	36.4	(α)1.57/1.86(β)	39.7	(α)1.49/1.82(β)	39.6	(α)1.56/1.82(β)
10	73.6		69.9		69.5	–
11	76.7	3.31	83.7	3.01	80.8	3.39
12	24.3	(β)1.81/2.11(α)	22.5	1.44/2.02	32.8	1.72/2.23
13	93.4	5.03	36.2	2.82/2.84	75.8	4.39
14	151.4		215.5		214.5	–
15	28.2	2.07	91.6		91.1	–
16	31.5	1.81/1.91	31.4	1.92/2.11	26.4	1.94 (2H)
17	26.6	1.69/1.82	26.5	1.72/1.91	32.1	1.98/2.26
18	86.4	3.91	86.4	4.04	86.4	4.08
19	83.8		84.0		83.9	–
20	34.5	1.66/2.01	34.5	1.72/1.90	35.1	1.78/1.87
21	26.1	1.85 (2H)	26.1	1.84/1.92	25.9	1.87 (2H)
22	87.4	3.76	87.7	3.76	88.7	3.86
23	70.4		70.4		70.9	–
24	24.0	1.12 (3H)	23.8	1.12 (3H)	23.6	1.16 (3H)
25	23.6	1.40 (3H)	23.5	1.40 (3H)	23.3	1.40 (3H)
26	20.1	1.21 (3H)	20.2	1.19 (3H)	20.3	1.19 (3H)
27	15.0	1.07 (3H)	20.1	1.14 (3H)	20.3	1.14 (3H)
28	66.7	3.49/3.63	66.3	3.55/3.68	66.1	3.58/3.76
29	24.5	1.23 (3H)	30.9	1.27 (3H)	25.6	1.37 (3H)
30	27.7	1.21 (3H)	27.7	1.19 (3H)	27.6	1.25 (3H)

The second compound, prethyrsenol A (**3**), was analyzed by HRESI-MS showing peaks at *m/z* 659.2217 and 661.3314 corresponding to a molecular formula of $C_{30}H_{53}BrO_9$. Analysis of the ^{1}H and ^{13}C NMR spectra, together with the interpretation of standard 2D NMR experiments (COSY, HSQC and HMBC) indicated that we were facing another structure related to thyrsenol A (**5**). However, **3** showed significant differences around the C-11 → C-15 fragment and at the C-28 position (Table 1). The COSY experiment established an ^{1}H–^{1}H spin-system H_2-11 (δ_H 3.01) → H_2-12 (δ_H 1.44 and 2.02) → H_2-13 (δ_H 2.82 and 2.84) that was connected, through the correlations of protons H_2-13 and H_2-28 (δ_H 3.55 and 3.68; J = 11.4 Hz) with C-14, the new carbonyl signal (δ_C 215.5) in the HMBC experiment. Careful comparison of ^{1}H and ^{13}C chemical shifts together with the dipolar correlations observed in the ROESY experiment of **3** with those of **2**, supports that both compounds possesses identical relative stereochemistry. In particular, the relative configuration of C-10 was thoroughly studied as the usual connection between rings B and C was broken at this point. Therefore, observation of dipolar correlations between H-7 (δ_H 2.95) and H-8α (δ_H 1.74), and this with H-11 (δ_H 3.01) confirmed the previous assumption. However the relative configurations at C-15 and C-18 could not be clearly established by using the NMR data. This problem was unequivocally solved by the addition of a small amount of acid to a sample of **3** which evolved into thyrsenol A (**5**), in a processes comparable to the acid conversion of erythromycin A and B in their corresponding enol ethers [10,11]. (Scheme 1).

The molecular formula ($C_{30}H_{53}BrO_{10}$) of the third new compound, 13-hydroxyprethyrsenol A (**4**), (HRESI-MS ion peaks $[M + Na-H_2O]^+$ at *m/z* 657.2614 and 659.2597), indicates the existance of an additional oxygen atom in comparison to prethyrsenol A (**3**). Comparison of the spectroscopic data of **3** and **4** only showed significant differences around the C-11 → C-13 spin-system, particularly in the

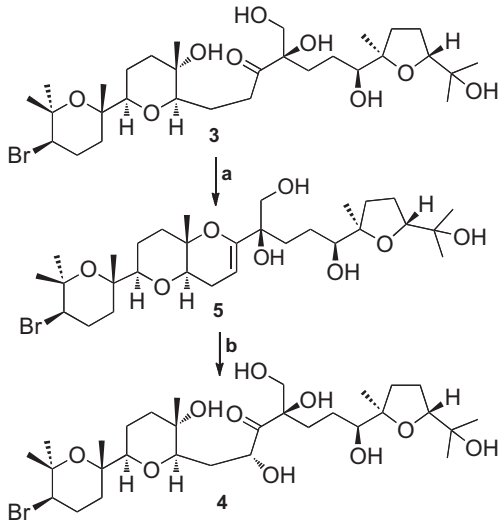

a: DOWEX 50, $CDCl_3$, rt, 2h; **b**: OsO_4, $CHCl_3$, rt, 2h

Scheme 1. Chemical correlations for compounds **3**–**5**.

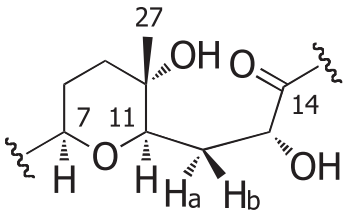

$^3J_{H\text{-}11—H\text{-}12a}$	*g*+	2.4
$^3J_{H\text{-}11—H\text{-}12b}$	*a*	9.6
$^3J_{C\text{-}13—H\text{-}11}$	*g*–	2.7
$^2J_{C\text{-}11—H\text{-}12b}$	*g*–	–5.8
$^2J_{C\text{-}11—H\text{-}12a}$	*a*	–1.8
$^3J_{H\text{-}13—H\text{-}12a}$	*a*	9.7
$^3J_{H\text{-}13—H\text{-}12b}$	*g*–	2.0
$^3J_{C\text{-}11—H\text{-}13}$	*g*–	2.4
$^2J_{C\text{-}13—H\text{-}12b}$	*a*	–2.0
$^2J_{C\text{-}13—H\text{-}12a}$	*g*+	–5.3

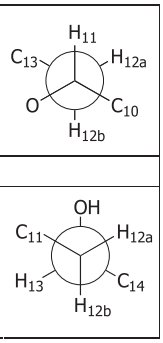

Fig. 2. *J*-Based configurational analysis for relative configuration at C-11/C-12 and C-12/C-13 bonds of 13-hydroxyprethyrsenol A (**4**) (*g* = *gauche; a* = *anti*).

chemical shifts of the H_2-13 methylene that change from δ_H 2.82 and 2.84 in **3** to a single proton signal centred at δ_H 4.39 in **4**. Moreover, this proton signal was correlated with a methine carbon at δ_C 75.8, indicating the presence of a secondary alcohol at carbon C-13. The other fragments of molecule showed identical connectivities in the COSY and HMBC experiments and almost superimposable chemical shifts to those observed for **3**. Again, the relative configurations of all chiral centres of **4**, with the exception of C-13, were proposed to be identical to those of **3** on the basis of a careful comparison of the ROESY experiment of both compounds. However, a different approach (*J*-based configurational analysis) was used to elucidate the relative configuration of C-13, as this chiral centre is located in an acyclic chain [12]. $^3J_{H,H}$ values were obtained from ^{1}H NMR and confirmed by a double resonance experiment, while $^{2,3}J_{C,H}$ values measured in an HSQC—HECADE spectrum [13]. The $^3J_{H,H}$ measured values indicated the existence of a single conformer around the C-11/C-12/C-13 bonds. Therefore, both H-12 protons could be located at their corresponding *anti* and *gauche* positions in each of the proposed conformers. Finally, from the measured $^{2,3}J_{C,H}$ values, particularly for $^2J_{C\text{-}11,H\text{-}12a}$ (−1.8 Hz) and $^2J_{C\text{-}13,H\text{-}12a}$ (−5.3 Hz), the relative configuration of C-13 was assigned as *R** in connection with C-11 (Fig. 2). Ultimately, it has to be noted that the previous structural proposal was confirmed by chemical transformation of a sample of thyrsenol A (**5**) in a compound identical in all respect to **4** by treatment with OsO_4 (Scheme 1).

3. Pharmacological evaluation

This class of polyether squalene natural products shows a variety of biological properties where its cytotoxicity against breast cancer cells is highly significant [5,14,15]. Therefore, the *in vitro* cytotoxic activity of **2**–**4** was assessed by XTT assays using a number of human cancer cells, including Jurkat, MM144, HeLa and CADO-ES-1 cell lines [16,17]. As shown in Table 2, Jurkat leukaemic cells were the most sensitive cells to the distinct polyether compounds. Interestingly, compound 13-hydroxyprethyrsenol (**4**) showed the highest effectiveness against CADO-ES-1 cell line (IC_{50}, 3.10 μM), being 5-fold more active than prethyrsenol and 15-dehydrothyrsenol A (**2**) (IC_{50}, 17 μM and 16 μM, respectively). However, one of the main problems that we came across in the course of all our biological evaluation tests was the poor water solubility of these compounds. In order to overcome solubility issues, we decided to synthesize a series of water-soluble derivatives through oxidation of the Δ15—28 olefin of **1** [18], followed by sulfonation of the resulting hydroxyl groups [19]. Thus, treatment of **1** with OsO_4 yielded **6** which was subsequently sulfonated by the action of SO_3-Pyridine to afford **7**. In a similar way, the hydroxy group at C-18 in **1** was sulfonated to afford **8** that was treated with NMO and OsO_4 to yield **9** (Scheme 2).

In all cases we observed a substantial improvement in water solubility, as expected on the basis of their calculated partition coefficients (Table 2), but this behaviour was not correlated with the potency of the compounds. In fact only a small effect was observed in the IC_{50} against Jurkat cell line. On the other hand, the introduction of a diol moiety at Δ15—28 olefin of **1** slightly increased the cytotoxic activity, and **6** resulted in a more selectivity against Jurkat cell line (Table 2).

In a previous work, we demonstrated that **1** targets integrins by a still uncertain mechanism. However it was clear that **1** significantly reduced the adhesion of breast cancer cells to immobilized extracellular matrix through the VLA integrins [8]. In addition it was found that **1** did not modify either the expression levels or the

Table 2
In vitro growth inhibitory activity of polyether compounds on tumour cells.[a]

IC_{50} (μM)					
Compound	ClogP	Jurkat	MM144	HeLa	CADO-ES-1
1	4.26	13.50 ± 2.12	21.50 ± 2.12	34.50 ± 2.12	12.00 ± 1.41
2	2.66	7.55 ± 2.05	7.30 ± 1.13	23.00 ± 1.41	16.50 ± 0.71
3	3.60	8.15 ± 2.62	10.20 ± 3.96	29.00 ± 1.41	14.50 ± 3.54
4	1.64	7.20 ± 3.96	15.50 ± 3.54	26.00 ± 2.83	3.10 ± 0.28
6	2.26	4.60 ± 0.85	21.00 ± 8.49	24.00 ± 2.83	18.00 ± 2.83
7	−1.77	8.60 ± 3.39	31.50 ± 6.36	35.50 ± 2.12	17.00 ± 1.41
8	2.24	12.00 ± 1.41	18.00 ± 1.41	33.00 ± 2.83	27.00 ± 5.66
9	0.24	6.90 ± 3.82	13.50 ± 4.95	27.50 ± 2.12	11.00 ± 1.41

[a] Growth inhibitory activity of polyether compounds against Jurkat T-cell acute leukaemia, MM144 multiple myeloma, HeLa epitheloid cervix carcinoma, and CADO-ES-1 Ewing's sarcoma, was determined using the XTT assay as described in Materials and Methods Data are shown as the mean values ± S.D. of three experiments performed in triplicate.

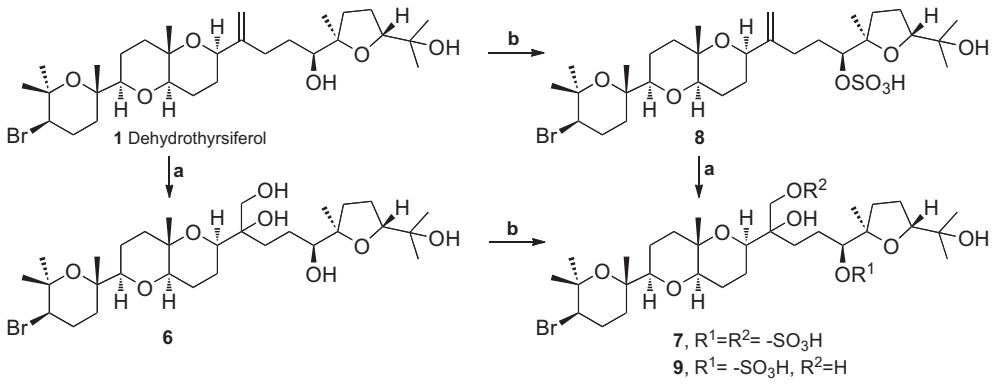

Scheme 2. Chemical modifications of dehydrothyrsiferol (**1**).

cell surface distribution of the integrins and that this compound preferentially targets these proteins in their high affinity state, interfering breast tumour cell signalling.

The fact that even large changes in the partition coefficients within the series of tested compounds, and expectedly in their ability to cross cellular membranes, did not produce changes in their bioactivity is in accordance with the indication that their target could be in the extracellular part of the cells, as it is the case for integrins. In addition the fact that those compounds with two or more adjacent hydroxyl groups exhibited the best bioactivities, could be a consequence of their ability to coordinate a metal ion located in the metal ion dependent adhesion site (MIDAS) of many integrins, providing them a better binding affinity for their targets.

4. Molecular docking

In order to find additional support for the previous hypothesis, i.e. the possibility that our compounds bind integrins at their MIDAS portion, and to identify the possible binding orientations of our compounds, docking simulations were undertaken using the Autodock Vina software [20]. Compounds **1**–**4** and **6**–**9** were docked onto the RGD binding site of the crystallographic structure of the αvβ3 integrin as it has been implicated in multiple aspects of tumour progression and metastasis [21–23]. A number of feasible bound conformations were generated and those with the most favourable binding energies were selected. Analysis of the modelling results, allowed us to differentiate two clusters of compounds based on their bound conformation: cluster A comprising structures **2**–**4**, **6**, and **9** (all with a primary alcohol at carbon C-28) and cluster B including molecules **1**, **7** and **8** (Fig. 3). Hence, while in the crystallographic structure of αvβ3 integrin in complex with the cyclic RGD tripeptide, the ligand interacts with the α and β chains of the protein, in our simulations the ligands are oriented in a more extended fashion, interacting mainly with the β chain as it have been predicted for other linear inhibitors [24].

In addition, from the analysis of the biological tests undertaken, we found that these compounds induced apoptosis. This fact was assessed by the appearance of a sub-G_1 region, representing apoptotic cells undergoing DNA breakdown, in cell cycle analysis by flow cytometry (Fig. 4). Further analysis of the biological activity of the new compounds was assessed using one of the main targets of squalene-derived polyether, the serine-threonine protein phosphatase type 2A. However, our *in vitro* assays showed that these compounds were inactive against PP2A at concentrations lower than 100 μM.

5. Conclusion

In the present study, we have identified three new cytotoxic compounds (**2**–**4**) structurally related to **1**, a natural product that has exhibet integrin inhibitory activity as a pausible mechanism for

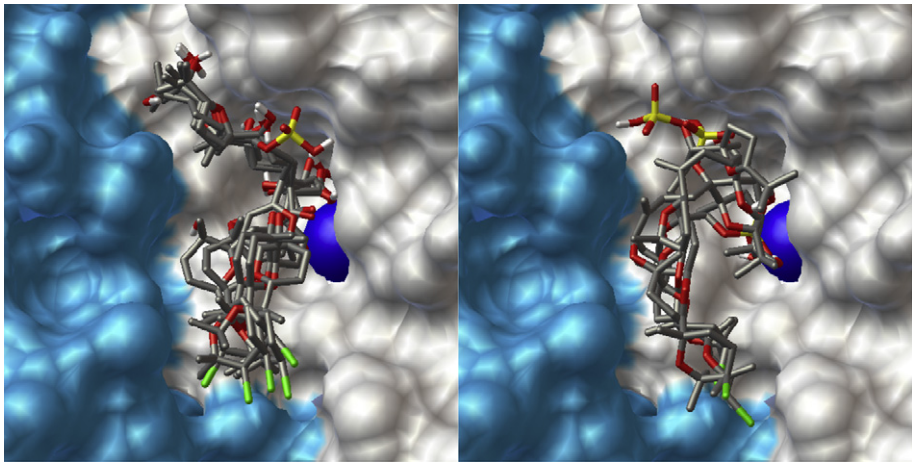

Fig. 3. Predict conformation of docking poliether compounds (*left*: cluster A, compouds **2**–**4**, **6**, and **9**; *rigth*: cluster B, compouds **1**, **7** and **8**) in the αvβ3 integrin active site. The turquoise and grey represent de α and β chain of the $\alpha_v\beta_3$ receptor and the Mn^{+2} is shown as blue sphere. (For interpretation of the references to colour in this figure legend, the reader is referred to the web version of this article.)

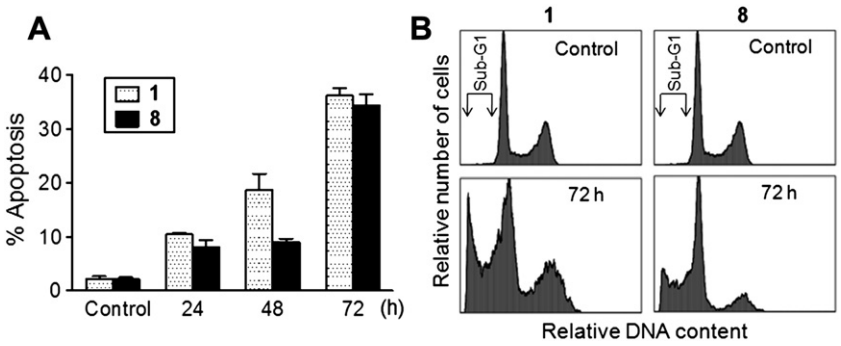

Fig. 4. Induction of apoptosis in Jurkat cells by compounds 1 and 8. (A) Jurkat cells were treated with 20 μM compounds 1 or 8 for the indicated times, and apoptosis was quantitated as the percentage of cells in the sub-G1 region in cell cycle analysis by flow cytometry. Untreated control cells were run in parallel. Data shown are means ± SD of 3 independent determinations. (B) Representative histograms of the relative DNA content in the distinct phases of cell cycle in untreated control Jurkat cells and after treatment with 20 μM compounds 1 and 8 for 72 h. The position of the sub-G1 region (hypodiploidy), integrated by apoptotic, cell is indicated by arrows.

its antitumour activity. In addition, four derivatives (**6**–**9**) were synthesized to improve the solubility and cytotoxicity of the isolated natural products. Thus, in order to overcome one of the main limitations of the lead **1** (i.e. its very low hydrosolubility) two water-soluble compounds, **7** and **9** were prepared by addition of sulfate groups. More importantly, it turned out that important changes in partition coefficients were achieved without any loss in activity. Finally, a ligand–receptor model has been proposed using a molecular modelling approach. Our results showed that the ligand bound poses obtained for compounds with the primary alcohol moiety at C-28 can be clustered into a single group which is similar to other inhibitors of integrins [24]. In addition, it appears that the interaction between this alcohol moiety with the metal ion seems to be crucial, while addition of a sulfate group at the C-18 position can be used to modulate the solubility of these compounds without important consequences in their bioactivity. Thus we have probed that it is possible to modulate the hydrophobicity of the lead **1** by addition of different water-solubilizing groups at different positions within a wide range of ClogP values (from −1.77 up to 4.26) maintaining or improving its bioactivity on tumour cells opening a better way to test these compounds *in vivo*.

6. Experimental section

6.1. General methods

Optical rotation was determined on a Perkin–Elmer 241 polarimeter using a sodium lamp operating at 589 nm. The IR spectrum was measured on a Bruker IFS55 spectrometer using a chloroform solution over a NaCl disk. NMR spectra were performed on Bruker AVANCE 400, 500 or 600 MHz instruments at 298 K, and coupling constants are given in Hz. COSY, 1D/2D TOCSY, HSQC, HMBC, and ROESY experiments were performed using standard pulse sequences. Phase-sensitive ROESY spectra were measured using a mixing time of 500 ms. $^{3}J_{H,H}$ values were measured from 1D ^{1}H NMR and when signal overlapping not permitted it, from the TOCSY. Data were processed using Topspin or MestReC software. Mass spectra were recorded on a VG AutoSpec FISON spectrometer. TLC was performed on Si gel Merck 60 F254, and TLC plates were visualized by spraying with phosphomolybdic acid reagent and heating.

6.2. Plant material

Specimes of *L. viridis* were collected in April 2008 in the intertidal zone at Callao Salvaje, Paraiso Floral, El Palmar (Tenerife, Canary Islands). Dried material from the sterile plants, sporophytes and gametophytes was filed at TFC Phyc. (Herbario de la Universidad de La Laguna, Departamento de Biología Vegetal, Botánica, Tenerife).

6.3. Extraction and chromatographic separation

The fresh alga was extracted with a 1:1 mixture of $CHCl_3$:CH_3OH at room temperature. The extract was evaporated *in vacuo* to leave a dark-green viscous oil (83.0 g, 1.5% dry weight). The crude extract was chromatographed on a Sephadex LH-20 column using $CHCl_3$–CH_3OH (1:1). Fractions that were similar in composition as shown by TLC were combined to give four fractions. The second fraction (53.4 g) was further separated by silica gel column eluted with increasing concentrations of ethyl acetate in *n*-hexane. The second fraction (0.219 g) was chromatographed again using a medium pressure silica gel chromatography Lobar LiChroprep-RP18 with CH_3OH:H_2O (9:1) as eluent. Final purification was carried out by HPLC employing a μ-Porasil column and using *n*-hexane:ethyl acetate or *n*-hexane:acetone in different proportions affording the pure new compounds, 15-dehydroxythyrsenol A (**2**) (0.56 mg); prethyrsenol A (**3**) (1.9 mg) and 13-hydroxyprethyrsenol A (**4**) (1.6 mg).

6.3.1. 15-Dehydroxythyrsenol A (*2*)

Amorphous white solid; $[\alpha]^{25}_{D}$ +21.4 (*c* 0.06, $CHCl_3$); IR ν_{max} ($CHCl_3$) 3437, 2927, 2857, 1677, 1457, 1376 and 1100 cm^{-1}; ESI-MS m/*z* 604, 602, 584, 580, 572, 413 and 301; HRESI-MS m/*z* 602.2810 (calcd for 602.2818, $C_{30}H_{51}O_7{}^{79}Br$, $[M]^+$); NMR data (500 MHz, $CDCl_3$) see Table 1.

6.3.2. Prethyrsenol A (*3*)

Amorphous white solid; $[\alpha]^{25}_{D}$ +6.3 (*c* 0.19, $CHCl_3$); IR ν_{max} ($CHCl_3$) 3420, 2972, 2860, 1711, 1649, 1378 and 1098 cm^{-1}; ESI-MS m/*z* 661, 659, 643, 641, 532, 531, 413 and 301; HRESI-MS m/*z* 659.2217 (calcd for 659.2760, $C_{30}H_{53}O_9{}^{79}BrNa$, $[M + Na]^+$); ^{1}H NMR data (400 MHz, $CDCl_3$) see Table 1.

6.3.3. 13-Hydroxyprethyrsenol A (*4*)

Amorphous white solid; $[\alpha]^{25}_{D}$ +27.1 (*c* 0.16, $CHCl_3$); IR ν_{max} ($CHCl_3$) 3396, 2928, 2868, 1712, 1457, 1377, 1129 and 1060 cm^{-1}; ESI-MS (NBA) *m/z* 659, 657, 606, 605, 577 and 413; HRESI-MS m/*z* 657.2614 (calcd 659.2614, $C_{30}H_{51}O_9{}^{79}BrNa$, $[M–H_2O + Na]^+$); NMR data (400 MHz, $CDCl_3$) see Table 1.

6.4. Chemical modifications

6.4.1. Transformation of prethyrsenol A (*3*) into thyrsenol A (*5*)

DOWEX-50 were added to a solution of **3** (1 mg) in $CDCl_3$ (1 mL), and the resulting mixture stirred for 2 h at room temperature,

monitoring the reaction by NMR. The resulting material was separated by HPLC chromatography (μ-Porasil column, n-Hex:-Acetone 4:1, flow rate 1 mL/min), obtaining 0.4 mg of pure **5**.

*6.4.2. Transformation of thyrsenol A (**5**) into 13-hydroxyprethyrsenol A (**4**)*

To a solution of **2** (1.5 mg) in $CHCl_3$ (0.5 mL), a catalytic solution of OsO_4 in t-BuOH was added and the resulting mixture was stirred for 2 h at room temperature. Afterwards, the solution was filtered off and concentrated to give a crude extract, which was chromatographed in HPLC (μ-Porasil column, n-Hex:Acetone 4:1, flow rate 1 mL/min), affording 0.6 mg of the compound **4**.

6.4.3. Synthesis of diol-compounds

To N-Methylmorpholine-N-Oxide (NMO, 24 mg, 0.205 mmol) in acetone:H_2O mixture (4:1; 3 mL) was added a catalytic OsO_4, and dehydrothyrsiferol (**1**) (20 mg, 0.034 mmol) in acetone (2 mL). The reaction was stirred for 24 h at room temperature. The excess OsO_4 was quenched by addition of $NaHCO_3$ (2 mg, 0.024 mmol) and the solvent mixture was removed *in vacuo*. The residue was purified by Sephadex LH-20 column ($CHCl_3$:MeOH 1:1) followed by an HPLC (μ-Porasil column; n-Hex:AcOEt:MeOH 14:5:1 as eluent; 0.75 mL/min flow rate) to give **6** (15 mg, 0.024 mmol) (yield: 70%). By the same reaction conditions, compound **8** (7 mg, 0.010 mmol) was converted to **9** (4 mg, 0.006 mmol) (yield: 60%). Compound **6**: ^{1}H NMR (600 MHz, $CDCl_3$): δ 1.14 (s, H_3-24), 1.16 (s, H_3-29), 1.20 (s, H_3-26), 1.21 (s, H_3-30), 1.23 (s, H_3-27), 1.28 (s, H_3-1), 1.35 (H-17), 1.40 (s, H_3-25), 1.43 (H-8), 1.52 (H-16), 1.53 (H-9), 1.53 (H-12), 1.54 (H-5), 1.60 (H-20), 1.65 (H′-17), 1.75 (H′-16), 1.76 (H′-8), 1.78 (H′-9), 1.79 (H-13), 1.81 (H′-5), 1.84 (H_2-21), 1.92 (H′-12), 1.96 (H′-13), 2.11 (H-4), 2.11 (H′-20), 2.25 (H′-4), 3.07 (dd, J = 1.9, 11.4 Hz, H-7), 3.45 (d, J = 11.3, H-28), 3.48 (dd, J = 1.3, 9.7 Hz, H-18), 3.61 (dd, J = 8.1, 12.5 Hz, H-11), 3.73 (d, J = 11.3 Hz, H′-28), 3.77 (dd, J = 5.8, 10.1 Hz, H-22), 3.90 (dd, J = 4.0, 12.3 Hz, H-3), 3.96 (dd, J = 2.5, 12.6 Hz, H-14). ^{13}C NMR (150 MHz, $CDCl_3$) δ 20.1 (C-26), 21.0 (C-12), 21.1 (C-13), 21.4 (C-27), 23.0 (C-8), 23.6 (C-25), 23.9 (C-24), 23.9 (C-29), 24.8 (C-17), 26.3 (C-21), 27.7 (C-30), 28.3 (C-4), 30.6 (C-16), 31.0 (C-1), 31.7 (C-20), 37.0 (C-5), 38.5 (C-9), 59.0 (C-3), 65.3 (C-28), 70.7 (C-23), 72.7 (C-10), 74.4 (C-6), 75.0 (C-2), 75.3 (C-15), 75.9 (C-11), 76.1 (C-14), 77.5 (C-18), 86.1 (C-19), 86.7 (C-7), 87.6 (C-22). Compound **9**: ^{1}H NMR (600 MHz, CD_3OD): δ 1.13 (s, H_3-24), 1.15 (s, H_3-30), 1.20 (s, H_3-29), 1.21 (s, H_3-27), 1.22 (s, H_3-26), 1.27 (s, H_3-1), 1.40 (s, H_3-25), 1.45 (H-8), 1.50 (H-12), 1.59 (H-9), 1.60 (H-5), 1.65 (H-20), 1.72 (H′-8), 1.75 (H′-9), 1.75 (H-17), 1.78 (H′-5), 17.8 (H-13), 1.79 (H-21), 1.89 (H′-17), 1.90 (H′-12), 1.91 (H′-21), 1.95 (H′-13), 2.09 (H-4), 2.28 (H′-4), 2.34 (H′-20), 3.10 (dd, J = 2.4, 11.3 Hz, H-7), 3.45 (d, J = 11.6 Hz, H-28), 3.56 (d, J = 11.6 Hz, H′-28), 3.64 (dd, J = 7.3, 11.0 Hz, H-11), 3.82 (dd, J = 6.7, 8.4 Hz, H-22), 3.95 (dd, J = 1.8, 11.9 Hz, H-14) 3.98 (dd, J = 3.6, 12.0 Hz, H-3), 4.25 (t, J = 4.3 Hz, H-18). ^{13}C NMR (150 MHz, CD_3OD) δ 19.6 (C-27), 20.0 (C-26), 21.0 (C-13), 21.3 (C-12), 21.5 (C-29), 23.2 (C-25), 23.3 (C-8), 24.6 (C-24), 25.5 (C-30), 27.5 (C-21), 28.4 (C-4), 29.3 (C-16), 30.6 (C-1), 35.8 (C-20), 37.0 (C-5), 39.1 (C-9), 59.0 (C-3), 64.6 (C-28), 71.3 (C-23), 72.2 (C-10), 73.7 (C-14), 75.3 (C-159), 74.8 (C-6), 75.2 (C-2), 76.8 (C-11), 84.3 (C-18), 85.2 (C-19), 86.6 (C-22), 86.8 (C-7). (C-16).

6.4.4. Preparation of sulfate compounds

To a solution of dehydrothyrsiferol (**1**) (20 mg, 0.034 mmol) in pyridine (5 mL) was added SO_3-pyridine complex (55.7 mg, 0.35 mmol) at room temperature. After stirring at 80 °C for 3 h, the reaction mixture was quenched with MeOH. Removal of the solvent gave a residue, which was purified by Sephadex LH-20 column ($CHCl_3$:MeOH 1:1) followed by an HPLC chromatography (XTerra column, MeOH:H_2O 17:3 as eluent and 1.5 mL/min flow rate) afforded **8** (14 mg, 021 mmol) (yield: 62%). By the same processes, **6** (7 mg, 0.011 mmol) was converted to **7** (3 mg, 0.004 mmol) (yield: 36%). Compound **8**: ^{1}H NMR (600 MHz, $CDCl_3$): δ 1.18 (s, H_3-24), 1.18 (s, H_3-26), 1.18 (s H_3-30), 1.21 (s, H_3-29), 1.21 (s H_3-27), 1.26 (s, H_3-1), 1.39 (s, H_3-25), 1.45 (H-8), 1.50 (H-9), 1.50 (H-21), 1.54 (H-5), 1.56 (H-12), 1.57 (H-20), 1.72 (H′-8), 1.76 (H′-12), 1.77 (H′-9), 1.80 (H′-21), 1.81 (H′-5), 1.82 (H-13), 1.99 (H′-13), 2.10 (H-4), 2.23 (H′-4), 2.23 (H-16), 2.27 (H′-20), 2.40 (H′-16), 3.07 (dd, J = 2.1, 11.1 Hz, H-7), 3.41 (dd, J = 5.7, 11.3 Hz, H-11), 3.89 (dd, J = 4.1, 12.3 Hz, H-3), 4.06 (H-22), 4.23 (dd, J = 4.0, 8.3 Hz, H-14), 4.54 (H-18), 4.83 (bs, H-28), 5.01 (bs, H′-28). ^{13}C NMR (150 MHz, $CDCl_3$): δ 19.6 (C-27), 20.3 (C-26), 21.3 (C-24), 21.3 (C-30), 21.8 (C-12), 23.1 (C-8), 23.7 (C-25), 25.3 (C-29), 26.6 (C-13), 28.1 (C-21), 28.4 (C-4), 28.4 (C-16), 30.9 (C-1), 30.9 (C-17), 31.5 (C-20), 37.4 (C-5), 38.7 (C-9), 59.0 (C-3), 72.3 (C-23), 72.5 (C-14), 72.8 (C-10), 74.2 (C-6), 74.8 (C-2), 78.7 (C-11), 83.6 (C-18), 85.4 (C-19), 86.5 (C-7), 87.1 (C-22), 109.2 (C-28), 151.4 (C-15). Compound **7**: ^{1}H NMR (600 MHz, CD_3OD): δ 1.13 (s, H_3-24), 1.14 (s, H_3-29), 1.17 (s, H_3-30), 1.21 (s, H_3-7), 1.23 (s, H_3-26), 1.27 (s, H_3-1), 1.40 (s, H_3-25), 1.41 (H-17), 1.45 (H-8), 1.46 (H-9), 1.51 (H-12), 1.61 (H-5), 1.62 (H-20), 1.73 (H′-8), 1.74 (H′-9), 1.75 (H′-17), 1.79 (H′-5), 1.81 (H-13), 1.82 (H_2-21), 1.90 (H′-12), 1.99 (H′-13), 2.05 (H′-20), 2.09 (H-4), 2.23 (H-16), 2.28 (H′-4), 2.40 (H-16), 3.10 (dd, J = 2.1, 11.1 Hz, H-7), 3.36 (dd, J = 1.8, 10.3 Hz, H-18), 3.65 (dd, J = 5.7, 11.3 Hz, H-11), 3.78 (dd, J = 5.8, 9.8 Hz, H-22), 3.94 (H-28), 3.96 (dd, J = 4.0, 8.3 Hz, H-14), 3.98 (dd, J = 4.1, 12.3 Hz, H-3), 3.99 (H-28′). ^{13}C NMR (150 MHz, CD_3OD) δ 21.0 (C-26), 21.6 (C-27), 21.9 (C-12), 23.8 (C-29), 24.3 (C-8), 24.5 (C-25), 25.4 (C-24), 26.5 (C-17), 26.6 (C-13), 26.7 (C-30), 27.5 (C-21), 29.2 (C-4), 31.6 (C-1), 31.6 (C-16), 34.9 (C-20), 38.1 (C-5), 39.9 (C-9), 59.9 (C-3), 70.7 (C-28), 71.9 (C-14), 72.2 (C-23), 72.8 (C-10), 75.6 (C-6), 76.0 (C-2), 77.5 (C-11), 79.2 (C-18), 87.7 (C-7), 86.9 (C-19), 87.7 (C-22). C-15.

6.5. Cell culture

Human Jurkat (T-cell acute leukaemia), MM144 (multiple myeloma), HeLa (epitheloid cervix carcinoma), and CADO-ES-1 (Ewing's sarcoma) cells were cultured in RPMI-1640 (Jurkat, MM144, CADO-ES-1) or DMEM (HeLa) culture medium containing 10% (v/v) heat-inactivated foetal bovine serum (FBS), 2 mM L-glutamine, 100 U/ml penicillin, and 100 μg/ml streptomycin at 37 °C in air containing 95% humidity and 5% CO_2. Cells were periodically tested for *Mycoplasma* infection using the MycoAlert© Mycoplasma detection kit (Lonza, Basel, Switzerland) as well as the Venor©GeM Advance Mycoplasma PCR detection Kit (Minerva Biolabs, Berlin, Germany), and found to be negative.

6.6. Cell growth inhibition assay

The effect of the distinct compounds in the proliferation of human tumor cell lines (cytostatic activity) was determined as previously described by using the XTT (sodium 3′-[1-(phenylaminocarbonyl)-3,4-tetrazolium]-bis (4-methoxy-6-nitro) benzene sulfonic acid hydrate) cell proliferation kit (Roche Molecular Biochemicals, Mannheim, Germany) as previously described [16]. Cells ($1.5–5.0 \times 10^3$ in 100 μl) were incubated in RPMI-1640 (Jurkat, MM144, CADO-ES-1) or DMEM (HeLa) culture medium containing 10% heat-inactivated FBS, in the absence and in the presence of the indicated compounds at a concentration range of 10^{-4} to 10^{-9} M, in 96-well flat-bottomed microtiter plates, and following 72 h of incubation at 37 °C in a humidified atmosphere of air/CO_2 (19/1) the XTT assay was performed. Measurements were done in triplicate, and each experiment was repeated three times. The IC_{50} (50% inhibitory concentration) value, defined as the drug concentration required to cause 50% inhibition in the cellular proliferation with respect to the untreated controls, was determined for each compound.

6.7. DNA content analysis by flow cytometry

Cells were centrifuged at 1200 rpm for 10 min, and the pellet was resuspended and fixed overnight in 70% ethanol at 4 °C. Cells were washed with PBS, pelleted at 1200 rpm for 10 min, and resuspended in 400 μl of PBS containing RNAse (50 μg/ml) for 1 h at room temperature. Propidium iodide was added to a final concentration of 5 μg/ml, and cells were analyzed by fluorescence flow cytometry. Quantitation of apoptotic cells was calculated as the percentage of cells in the sub-G_1 region (hypodiploidy) in cell cycle analysis as previously described [17].

6.8. Protein phosphatase inhibition assays

Inhibitory activity against serine/threonine phosphatase type 2A was evaluated at 37 °C using 0.025 units/μL of purified $PP2A_c$ and 5 mM *p*-nitrophenyl phosphate (*p*NPP) as substrate. The reaction was monitored following by UV/visible absorption spectroscopy at 405 nm and data were fitted to a one-site binding model. Inhibitory assays with all compounds (**1**–**9**) were performed simultaneously in quintuplicate.

6.9. Docking studies

Docking simulations were performed with Autodock Vina software (v.1.1) using the GUI ADT (v.1.5.4). The receptor file was prepared using the coordinates of the extracellular segment of integrin αvβ3 in complex with an Arg-Gly-Asp ligand (1L5G) obtained from the Protein Data Bank in which the ligand was removed. The atomic charges of the manganese ions as well as that of those residues in their coordination spheres were not calculated as assigning atom charges is not needed by AutoDock Vina. Default parameters were used and changes in the exhaustiveness of the search did not modified the results significantly. The docking results were clustered on the basis of the RMSD between the coordinates of the atoms.

Acknowledgement

Financial support was provided by the grants CTQ2008-06754-C04-01 and SAF2008-02251 (MEC); C2008000145 and EXMAR (ACISII); RD06/0020/1037 from Red Temática de Investigación Cooperativa en Cáncer, Instituto de Salud Carlos III, co-funded by the Fondo Europeo de Desarrollo Regional of the European Union, and Junta de Castilla y León (GR15-Experimental Therapeutics and Translational Oncology Program, and Biomedicine Project 2009) and F.C.P. is the recipient of a SEGAI-ULL fellowship.

Appendix. Supplementary material

Supplementary data associated with this article can be found, in the online version, at doi:10.1016/j.ejmech.2011.04.051.

References

[1] G.M. Cragg, D.J. Newman, Nat. Prod. 70 (2007) 461–477.
[2] G.M. Cragg, P.G. Grothaus, D.J. Newman, Chem. Rev. 109 (2009) 3012–3043.
[3] D.J. Faulkner, Nat. Prod. Rep. 19 (2002) 1–48 (and previous reviews in this series).
[4] J.W. Blunt, B.R. Copp, M.H.G. Munro, P.T. Northcote, M.R. Prinsep, Nat. Prod. Rep. 28 (2011) 196–268 (and previous reviews in this series).
[5] J.J. Fernández, M.L. Souto, M. Norte, Nat. Prod. Rep. 17 (2000) 235–246.
[6] M.L. Souto, C.P. Manríquez, M. Norte, J.J. Fernández, Tetrahedron 58 (2002) 8119–8125.
[7] M.L. Souto, C.P. Manríquez, M. Norte, F. Leira, J.J. Fernández, Bioorg. Med. Chem. Lett. 13 (2003) 1261–1264.
[8] M.K. Pec, M. Artwohl, J.J. Fernández, M.L. Souto, T. Giradles, D. Alvarez de La Rosa, A. Valenzuela-Fernández, F. Díaz-González, Exp. Cell Res. 313 (2007) 1121–1134.
[9] M. Norte, J.J. Fernández, M.L. Souto, J.A. Gavín, M.D. García-Grávalos, Tetrahedron 53 (1997) 3173–3178.
[10] P. Kurath, P.H. Jones, R.S. Egan, T.J. Perun, Experientia 27 (1971) 362.
[11] L. Toscano, E. Seghetti, Tetrahedron Lett. 49 (1983) 5527–5530.
[12] N. Matsumori, D. Kaneno, M. Murata, H. Nakamura, K. Tachibana, J. Org. Chem. 64 (1999) 866–876.
[13] W. Kozminski, D. Nanz, J. Magn. Reson. 142 (2000) 294–299 Kozminski, W.; Nanz, D. J. Magn. Reson. 124 (1997) 383–392.
[14] M.K. Pec, A. Aguirre, K. Moser-Thier, J.J. Fernández, M.L. Souto, J. Dorta, F. Díaz-González, J. Villar, Biochem. Pharmacol. 65 (2003) 1451–1461.
[15] M.K. Pec, A. Aguirre, J.J. Fernández, M.L. Souto, J. Dorta, J. Villar, J. Int. J. Mol. Med. 10 (2002) 605–608.
[16] M.-H. David-Cordonnier, C. Gajate, O. Olmea, W. Laine, J. de la Iglesia-Vicente, C. Perez, C. Cuevas, G. Otero, I. Manzanares, C. Bailly, F. Mollinedo, Chem. Biol. 12 (2005) 1201–1210.
[17] C. Gajate, A.M. Santos-Beneit, A. Macho, M. Lazaro, A. Hernandez-De Rojas, M. Modolell, E. Munoz, F. Mollinedo, Int. J. Cancer 86 (2000) 208–218.
[18] S. Jew, E. Roh, E. Baek, L. Mireille, H. Kim, B. Jeong, M. Park, H. Park, Tetrahedron Asymetry 11 (2000) 3395–4218.
[19] H. Sato, T. Maeba, R. Yanase, A. Yamaji-Hasegawa, T. Kobayashi, N. Chida, J. Antibiot. 58 (2005) 37–49.
[20] O. Trott, A.J. Olson, J. Comp. Chem. 31 (2010) 455–461.
[21] P.C. Brooks, A.M.P. Montgomery, M. Rosenfeld, R.A. Reisfeld, T. Hu, G. Killer, D.A. Cheresh, Cell 79 (1994) 1157–1164.
[22] J. Xiong, T. Stehle, R. Zhang, A. Joachimiak, M. Frech, S.L. Goodman, M.A. Arnaout, Science 296 (2002) 151–155.
[23] D. Cox, M. Brennan, N. Moran, Nat. Rev. Drug Discov. 9 (2010) 804–820.
[24] R. Dayam, F. Aiello, J. Deng, Y. Wu, A. Garofalo, Z. Chen, N. Neamati, J. Med. Chem. 49 (2006) 4526–4532.